

First-principles study on lithium and magnesium nitrogen hydrides for hydrogen storage

T. Tsumuraya, T. Shishidou, T. Oguchi*

Department of Quantum Matter, ADSM, Hiroshima University, Higashihiroshima 739-8530, Japan

Received 24 October 2006; received in revised form 27 February 2007; accepted 28 February 2007

Available online 12 March 2007

Abstract

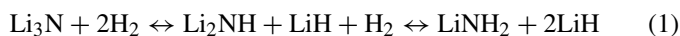
We have investigated the fundamental properties such as structural stability, heat of formation and electronic structure of lithium and magnesium nitrogen hydrides, LiNH_2 , $\text{Mg}(\text{NH}_2)_2$ and Li_2NH , by means of the first-principles calculations using highly precise all-electron full-potential linear augmented plane wave method. The heats of formation involved in the reactions $\text{Li}_2\text{NH} + \text{H}_2 \leftrightarrow \text{LiNH}_2 + \text{LiH}$ are estimated as -63 kJ/mol H_2 within generalized gradient approximation and -71 kJ/mol H_2 within local density approximation. Furthermore, we also obtain heats of formation concerning two elementary reactions given by an ammonia mediated model for H_2 desorption mechanism.

© 2007 Elsevier B.V. All rights reserved.

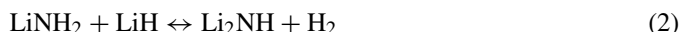
Keywords: Energy storage materials; Solid state reactions; Enthalpy; Crystal structure; First-principles calculation

1. Introduction

One of the problems related to the employment of hydrogen-based fuel cells for vehicular transportation is “on-board” hydrogen storage. Hydrogen storage in solids has long been recognized as one of the most practical approach for this purpose. Chen et al. have shown that lithium nitride Li_3N can absorb/desorb hydrogen in the following two-step reversible reaction with gaseous hydrogen without any catalyst [1]:



Theoretically, 10.4 mass% hydrogen can be reversibly stored in this reaction. Ichikawa et al. have investigated the mixture of lithium amide LiNH_2 and lithium hydride LiH doped a small amount (1 mol%) of titanium chloride TiCl_3 as a catalyst to improve the reaction kinetics in the second step of the reaction [2]:

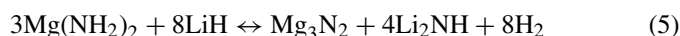


The mechanism of the desorption reaction (2) has been experimentally examined in detail [3,4]. Ichikawa et al. have proposed

that the reaction progressed by two elemental reactions mediated by ammonia molecule NH_3 :



Quite recently, some new systems have developed that several types of magnesium hydrides substitute for lithium hydride systems. For instance, Leng et al. have investigated a composite material made by ball milling of 3:8 molar mixture of $\text{Mg}(\text{NH}_2)_2$ and LiH under 1.0 MPa H_2 atmosphere and proposed the following reversible reaction [5]:



The experimental results show that a large amount of hydrogen (7 mass%) start to be desorbed at 140°C and a desorption peak at 190°C is formed, without any catalyst used. The hydrogenating and dehydrogenating reaction mechanism and fundamental properties of these hydrides still remain as a matter to be investigated. In particular, the crystal structure of lithium imide Li_2NH is not fully determined yet. In this paper, we discuss the heats of formation in the reactions (1)–(4) and the fundamental properties of LiNH_2 , $\text{Mg}(\text{NH}_2)_2$ and Li_2NH , on the basis of the first-principles calculations using all-electron full-potential linear augmented plane wave (FLAPW) method.

* Corresponding author. Fax: +81 82 424 7014.

E-mail address: oguchi@hiroshima-u.ac.jp (T. Oguchi).

2. Computational methods

Our first-principles calculations are based on the local spin density approximation (LSDA) or generalized gradient approximation (GGA) to density functional theory. Kohn–Sham equations are self-consistently solved in a scalar-relativistic fashion by using FLAPW method. Uniform k mesh sets of $4 \times 4 \times 4$ for LiNH_2 , $4 \times 4 \times 4$ for Li_2NH , $3 \times 3 \times 3$ for $\text{Mg}(\text{NH}_2)_2$, $12 \times 12 \times 12$ for LiH , and $6 \times 6 \times 6$ for Li_3N are adopted. Common muffin–tin sphere radii are set to be 0.8, 0.55, and 0.35 Å for Li, N and H, respectively, for all compounds and gases. We have checked convergence of the plane-wave cutoffs for the wavefunctions and the electron density. For molecule and isolated atom calculations, we use a bcc supercell with $a = 8$ Å and a Γ -point k sampling.

3. Results and discussion

3.1. Crystal structure

To obtain the heat of formation from first-principles calculations, information on the stable crystal structure is indispensable. We have performed structural optimization in advance for all solids and gases involved in the reactions. Calculated equilibrium lattice constants are listed in Table 1. Theoretical lattice constants are generally in good agreement with experiment. Quantitatively better agreement has been attained by using GGA. The crystal structure of Li_3N , LiH , LiNH_2 and $\text{Mg}(\text{NH}_2)_2$ have been already determined quite accurately by X-ray and/or neutron diffraction experiments, whereas that of Li_2NH has never been fully determined yet as shall be discussed below. Crystal structure of Li_3N is hexagonal (space group $P6/mmm$), LiNH_2 is tetragonal ($I\bar{4}$) [6,7,9], LiH is cubic ($Fm\bar{3}m$), Li metal is cubic ($Im\bar{3}m$) and $\text{Mg}(\text{NH}_2)_2$ is tetragonal ($I4_1/acd$) [8,9].

3.1.1. LiNH_2 and $\text{Mg}(\text{NH}_2)_2$

In LiNH_2 , all of the Li^+ ions are coordinated by four amide ions $(\text{NH}_2)^-$. For LiNH_2 , we have determined firstly unitcell volume by keeping the c/a ratio constant at the experimental value, and then the c/a ratio for the obtained equilibrium volume. For $\text{Mg}(\text{NH}_2)_2$, we have used experimentally determined

Table 2
Bond lengths and angles

| | LiNH_2 | Li_2NH | $\text{Mg}(\text{NH}_2)_2$ |
|----------------------------|-----------------|------------------------|----------------------------|
| LDA | | | |
| $d(\text{N}-\text{H})$ (Å) | 1.034, 1.036 | 1.040 | 1.044 |
| $\angle\text{HNH}$ (°) | 103.1 | | 101.0 |
| GGA | | | |
| $d(\text{N}-\text{H})$ (Å) | 1.029, 1.031 | 1.035 | 1.031 |
| $\angle\text{HNH}$ (°) | 102.5 | | 101.4 |
| Experiments [9,13] | | | |
| $d(\text{N}-\text{H})$ (Å) | 0.967, 0.978 | 0.977 | 0.98, 1.07 |
| $\angle\text{HNH}$ (°) | 104.1 | | 107.2, 105.2, 101.1 |

lattice constants [9] ($a = 10.3758$ Å, $c = 20.062$ Å) and performed structural optimization with respect to the internal atomic positions. As a result, the bond length and angle between N and H are shown in Table 2. The bond length and angle in the amides are quite similar to those of H_2O molecule (0.957 Å and 104.5°). The results are consistent with the experimentally obtained structure. Optimized H–N–H bond angle of $\text{Mg}(\text{NH}_2)_2$ is a little bit smaller than that of LiNH_2 . In general, LDA predicts smaller volume in solids than GGA while both approximations lead to almost compatible bond lengths and angles, as shown in Tables 1 and 2.

3.1.2. Li_2NH

As for Li_2NH , the anti-fluorite crystal structure has been suggested in 1951, but hydrogen position has not been identified [10]. Recently, Ohyama et al. have performed neutron powder diffraction experiments for Li_2NH [11]. However, the hydrogen position is not well identified and they propose two models for the crystal structure. They have concluded that the $F\bar{4}3m$ structure is most probable. Noritake et al. have carried out X-ray powder diffraction experiments and concluded that the space group is $Fm\bar{3}m$ [12]. We have examined hydrogen positions starting from the anti-fluorite structure by using first-principles total-energy and atomic-force calculations and obtained that the most stable H position is along the $[001]$ direction from N at a distance of 1.04 Å, leading to a tetragonal system. Quite recently, Balogh et al. have made deuterated samples Li_2ND and performed neutron and X-ray powder diffraction experiments [13]. The resulting lattice constant is approximately twice as large as that reported previously. The H position is now determined, but eight Li atoms are missing. Herbst et al. have proposed orthorhombic $Ima2$ structure where the missing Li positions are determined using first-principles calculations [14]. We have calculated total-energy difference between the two tetragonal and orthorhombic crystal structures and obtained that the orthorhombic structure is more stable than the tetragonal one by 0.22 eV/f.u. In the following study, we assume the orthorhombic structure proposed by Herbst et al. for Li_2NH with the internal atomic positions relaxed within the present FLAPW method in order to evaluate the heat of formation.

Quite recently, several new structures have been predicted from first-principles calculations. Magyari–Kope et al. proposed orthorhombic structure ($Pnma$) [15]. Muller et al. proposed layered ($P\bar{1}$) and orthorhombic ($Pbca$) ones [16] and concluded

Table 1
Optimized structure together with the corresponding experimental data

| | | LDA | GGA | Exp. |
|-----------------------|----------------------------|---------|----------|---------|
| LiNH_2 | a (Å) | 4.79580 | 5.04830 | 5.03164 |
| | c (Å) | 9.97143 | 10.27835 | 10.2560 |
| | c/a | 2.0792 | 2.0360 | 2.0383 |
| Li_3N | a (Å) | 3.548 | 3.624 | 3.65 |
| | c (Å) | 3.794 | 3.866 | 3.88 |
| | c/a | 1.0693 | 1.0668 | 1.0630 |
| LiH | a (Å) | 3.90358 | 3.99983 | 4.076 |
| Li | a (Å) | 3.350 | 3.427 | 3.510 |
| H_2 | $d(\text{H}-\text{H})$ (Å) | 0.7738 | 0.7568 | 0.7414 |
| N_2 | $d(\text{N}-\text{N})$ (Å) | 1.099 | 1.110 | 1.10 |
| NH_3 | $d(\text{N}-\text{H})$ (Å) | 1.026 | 1.0257 | 1.012 |
| | $\angle\text{HNH}$ (°) | 106.5 | 106.5 | 106.7 |

Table 3
Energy differences for predicted structures of Li_2NH

| | ΔH_{el} | ΔE (kJ/mol) | ΔE (eV/f.u.) | V (a.u./f.u.) | PP ^a (kJ/mol) |
|------------------------------|------------------------|---------------------|----------------------|-----------------|--------------------------|
| Orthorhombic (<i>Ima2</i>) | -191.6 | 0 | 0 | 214 | 0 |
| Layered (<i>P1</i>) | -195.6 | -4.0 | -0.041 | 248 | -2.8 |
| Orthorhombic (<i>Pnma</i>) | -196.2 | -4.6 | -0.047 | 229 | -3.1 |
| Orthorhombic (<i>Pbca</i>) | -198.1 | -6.5 | -0.067 | 239 | -4.8 |

^a Pseudopotential results from Ref. [16].

that the most stable structure is orthorhombic (*Pbca*). However, energy differences between them are quite small. Our all-electron FLAPW results for the previously predicted structures are listed in Table 3. The present results are in good agreement with pseudopotential ones. The most stable structure is orthorhombic (*Pbca*) but energy differences to the other structures are not so large. The equilibrium volumes per formula unit in the newly predicted structures are likely overestimated compared with experiment while the orthorhombic (*Ima2*) structure has consistent volume [14] with experiment (216 a.u./f.u.) [13].

3.2. Electronic structure

Figs. 1–3 show total and partial electronic density of states (DOS) within GGA for LiNH_2 , $\text{Mg}(\text{NH}_2)_2$ and Li_2NH . Calculated energy gap is 3.21 eV for LiNH_2 , 3.02 eV for $\text{Mg}(\text{NH}_2)_2$ and 2.65 eV for Li_2NH . The most characteristic feature seen in DOS is that lithium and magnesium partial DOS's are quite small within the muffin–tin spheres in the valence and conduction band regions, though the magnesium partial DOS's are relatively larger than those of lithium in the valence bands. Therefore, these compounds may have almost ionic bonding: $\text{Li}^+[\text{NH}_2]^-$,

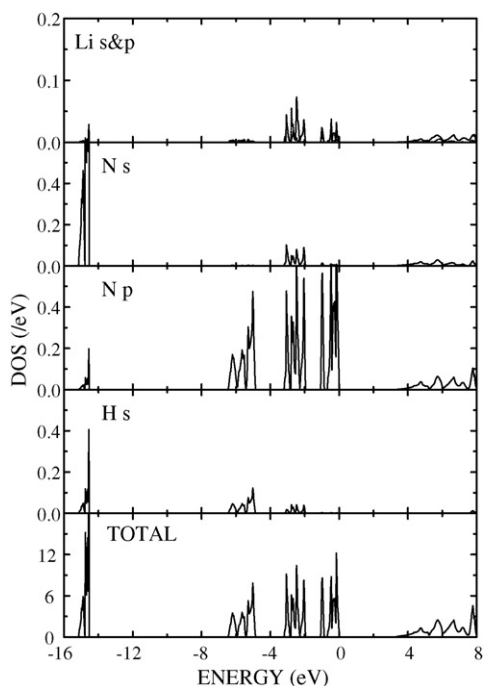


Fig. 1. Calculated partial density of states for LiNH_2 . The origin in energy is set to at the valence band maximum.

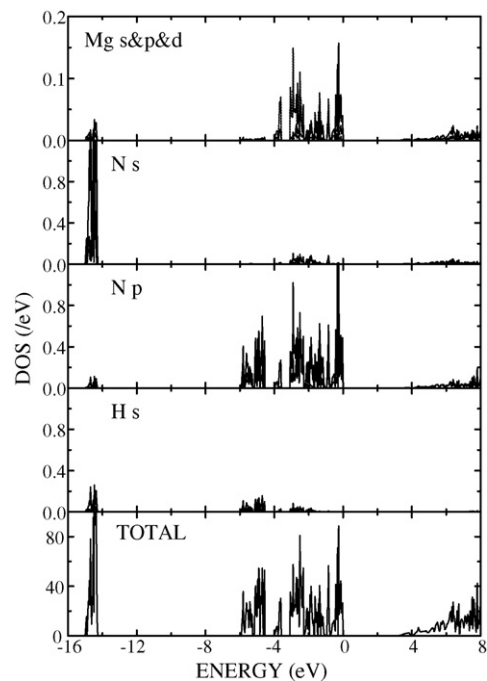


Fig. 2. Calculated partial density of states for $\text{Mg}(\text{NH}_2)_2$. The origin in energy is set to at the valence band maximum.

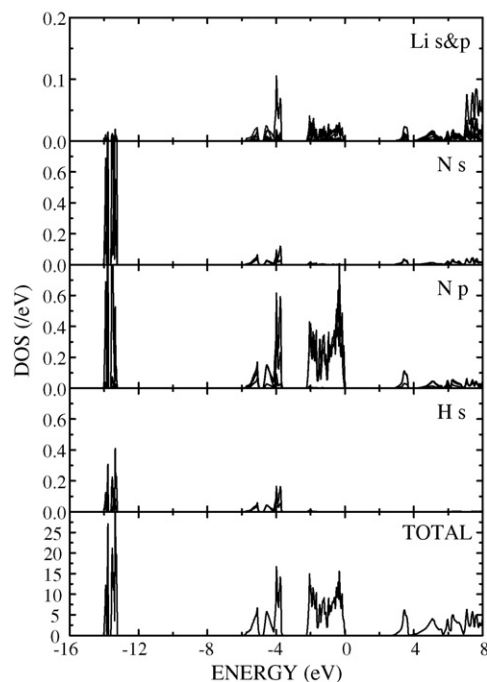


Fig. 3. Calculated partial density of states for Li_2NH . The origin in energy is set to at the valence band maximum.

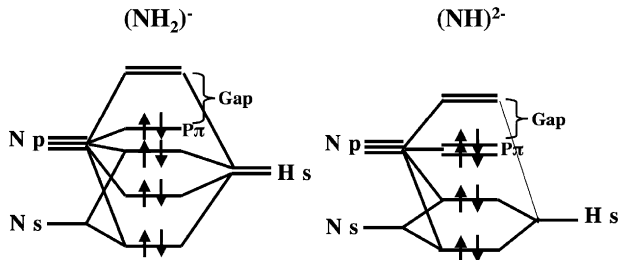


Fig. 4. Schematic energy diagram of amide $(\text{NH}_2)^-$ and imide NH^{2-} based on molecular-orbital model.

$(\text{Li}^+)_2[\text{NH}]^{2-}$, $\text{Mg}^{2+}[(\text{NH}_2)^{1-}]_2$. The valence bands are mostly composed of N s and p and H s states. In conjunction to this fact, DOS in the valence band region are quite similar in the amides LiNH_2 and $\text{Mg}(\text{NH}_2)_2$. The general features in DOS of the amide and imide can be understood by schematic energy diagrams described within molecular-orbital models for the isolated amide and imide molecules shown in Fig. 4. The most interesting common feature in the amide and imide is that the highest occupied states are of non-bonding made of N p_π orbitals.

3.3. Heats of formation

In order to study the phase stability of compounds involved in the reactions, it is quite useful to calculate heats of formation, which is the most fundamental and important quantities for hydrogen-storage materials. Heat of formation in compounds AB is defined as

$$\Delta H_{\text{el}} = E(AB) - E(A) - E(B) \quad (6)$$

where $E(A)$, $E(B)$ and $E(AB)$ are calculated total energies per formula unit of an elemental metal Li, molecules $\text{N}_2, \text{H}_2, \text{LiNH}_2, \text{Li}_2\text{NH}$. For example

$$\Delta H_{\text{el}}(\text{LiNH}_2) = E(\text{LiNH}_2) - E(\text{Li}) - \frac{1}{2}E(\text{N}_2) - E(\text{H}_2) \quad (7)$$

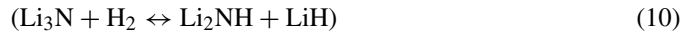
Table 4 shows heats of formation for each compound. We have carried out these calculations within both LDA and GGA. From the results that heats of formation for each compound and gas, we can estimate heats of formation (enthalpy change at ambient pressure) in the H absorption and desorption reactions. In these light-element H storage materials, the zero-point energy contribution ΔH_{ZPE} should be incorporated. In this paper, we show the heats of formation with the zero-point energies taken from some previous works by Herbst and Hector [14] and Miwa et al. [17]. We are now in progress to estimate the zero-point energy contribution by performing frozen phonon calculations. The electronic contribution ΔH_{el} to the heat of formation for each reaction is obtained within GGA. The heat

of formation in the whole reaction between the end materials (1) $(\text{Li}_3\text{N} + 2\text{H}_2 \leftrightarrow \text{LiNH}_2 + 2\text{LiH})$ is found to be

$$\Delta H_0 = \Delta H_{\text{el}} + \Delta H_{\text{ZPE}} = -85 \text{ kJ/mol H}_2 \quad (8)$$

$$\Delta H_{\text{el}} = -101 \text{ kJ/mol H}_2 \quad (9)$$

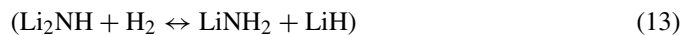
Miwa et al. have reported the heat of formation of -85 kJ/mol H_2 including the zero-point energy [17]. Our result is also in good agreement with the experimental value of -81 kJ/mol H_2 by Chen et al. [1]. We estimate the heats of formation by separating the whole reaction (1) into the two steps. The first reaction gives



$$\Delta H_0 = -108 \text{ kJ/mol H}_2 \quad (11)$$

$$\Delta H_{\text{el}} = -121 \text{ kJ/mol H}_2 \quad (12)$$

and the second reaction does



$$\Delta H_0 = -63 \text{ kJ/mol H}_2 \quad (14)$$

$$\Delta H_{\text{el}} = -81 \text{ kJ/mol H}_2 \quad (15)$$

LDA calculations for the whole reaction predict $\Delta H_0 = -71 \text{ kJ/mol H}_2$ with $\Delta H_{\text{el}} = -91 \text{ kJ/mol H}_2$. In this case, the zero point energy contribution is taken from the results by Herbst and Hector [14]. In addition, we estimate the heats of formation for the two elementary reactions mediated by ammonia (3) and (4)

$$\Delta H_{\text{el}} = -121 \text{ kJ/mol NH}_3 \text{ for (3)} \quad (16)$$

$$\Delta H_{\text{el}} = 40 \text{ kJ/mol NH}_3 \text{ for (4)} \quad (17)$$

The enthalpy change in LiNH_2 for releasing NH_3 is strongly endothermic. (The experimental value for the reaction is reported to be 84 kJ/mol NH_3 [2].) The another the reaction between LiH and NH_3 (4) is exothermic. Our results are consistent with experimental results. LiNH_2 solely desorbs NH_3 gas at much higher temperature than desorption temperature of H_2 from mixture of LiNH_2 and LiH . Experimentally, the thermal desorption mass spectroscopy (TDMS) measurements of ammonia from pure LiNH_2 show that the ammonia gas is drastically desorbed starting at 300°C , and the desorption peaked at 350°C [2]. It is also reported that gaseous hydrogen (5.5–6 mass%) between 150 and 250°C is reversibly desorbed/absorbed in a ball-milled mixture of LiNH_2 and LiH . Therefore, the existence of LiH is a crucial factor for H_2 desorption from compounds at low temperature.

4. Conclusions

Our first-principles calculations show that the most stable crystal structure of Li_2NH is orthorhombic (Pbca), though the other structures we studied are found to be almost equally stable. Electronic structure of $\text{Mg}(\text{NH}_2)_2$ is almost the same as that of LiNH_2 . The different feature in the electronic structure between $\text{Mg}(\text{NH}_2)_2$ and LiNH_2 is that hybridization between Mg and N 2p in $\text{Mg}(\text{NH}_2)_2$ is slightly stronger than in LiNH_2 . We have

Table 4
Calculated electronic contributions to the heats of formation ΔH_{el} in kJ/mol

| | Li_3N | LiNH_2 | LiH | Li_2NH |
|-----|-----------------------|-----------------|--------------|------------------------|
| LDA | -223.7 | -266.6 | -101.6 | -277.3 |
| GGA | -150.3 | -193.2 | -79.2 | -191.6 |

estimated the heats of formation in the reactions of Li–N–H systems. The heat of formation in the reaction $\text{Li}_2\text{NH} + \text{H}_2 \leftrightarrow \text{LiNH}_2 + \text{LiH}$ is -63 kJ/mol H_2 . It is found that the enthalpy change in LiNH_2 for releasing NH_3 is strongly endothermic while the reaction between LiH and NH_3 is exothermic.

Acknowledgements

This work is supported by the Grant of the NEDO project “Development for Safe Utilization and Infrastructure of Hydrogen Industrial Technology” and COE Research of the Ministry of Education, Culture, Sports, Science and Technology of Japan (MEXT).

References

- [1] P. Chen, Z. Xiong, J. Luo, J. Lin, K.L. Tan, *Nature* 420 (2002) 302.
- [2] T. Ichikawa, S. Isobe, N. Hanada, H. Fujii, *J. Alloys Compd.* 365 (2004) 271.
- [3] T. Ichikawa, N. Hanada, S. Isobe, H.Y. Leng, H. Fujii, *J. Phys. Chem. B* 108 (2004) 7887.
- [4] S. Isobe, T. Ichikawa, S. Hino, H. Fujii, *J. Phys. Chem. B* 109 (2005) 14855.
- [5] H.Y. Leng, T. Ichikawa, S. Hino, N. Hanada, S. Isobe, H. Fujii, *J. Phys. Chem. B* 108 (2004) 8763.
- [6] V.H. Jacobs, R. Juza, *Z. Anorg. Allg. Chem.* 391 (1972) 271.
- [7] M. Nagib, V.H. Jacobs, *Atomkernenergie* 21 (1973) 275.
- [8] V.H. Jacobs, *Z. Anorg. Allg. Chem.* 382 (1971) 97.
- [9] M.H. Sørby, Y. Nakamura, H.W. Bricks, S. Hino, H. Fujii, B.C. Hauback, *J. Alloys Compd.* 428 (2007) 297.
- [10] V.R. Juza, K. Opp, *Z. Anorg. Allg. Chem.* 266 (1951) 325.
- [11] T. Noritake, H. Nozaki, M. Aoki, S. Towata, G. Kitahara, Y. Nakamori, S. Orimo, *J. Alloys Compd.* 393 (2004) 271.
- [12] K. Ohyama, Y. Nakamori, S. Orimo, K. Yamada, *J. Phys. Soc. Jpn.* 74 (2005) 264.
- [13] M.P. Balogh, C.Y. Jones, J.F. Herbst, L.G. Hector, M. Kundrat Jr., *J. Alloys Compd.* 420 (2006) 326.
- [14] J.F. Herbst, L.G. Hector Jr., *Phys. Rev. B* 72 (2005) 125120.
- [15] B. Magyari-Kope, V. Ozolins, C. Wolverton, *Phys. Rev. B* 73 (2006) 220101.
- [16] T. Muller, G. Ceder, *Phys. Rev. B* 74 (2006) 134104.
- [17] K. Miwa, N. Ohba, Y. Nakamori, S. Orimo, *Phys. Rev. B* 71 (2005) 195109.